

# Reference Correlation for the Thermal Conductivity of Xenon from the Triple Point to 606 K and Pressures up to 400 MPa

Danai Velliadou<sup>1</sup>, Marc J. Assael<sup>1,a)</sup>, Konstantinos D. Antoniadis<sup>1</sup>,  
Marcia L. Huber<sup>2</sup>

<sup>1</sup> *Laboratory of Thermophysical Properties and Environmental Processes,  
Chemical Engineering Department, Aristotle University, Thessaloniki 54636, Greece*

<sup>2</sup> *Applied Chemicals and Materials Division, National Institute of Standards and Technology,  
325 Broadway, Boulder, CO 80305, USA*

A new wide-ranging correlation for the thermal conductivity of xenon, based on the most recent theoretical calculations and critically evaluated experimental data, is presented. The correlation is designed to be used with a high-accuracy Helmholtz equation of state, and it is valid from the triple-point temperature to 606 K and pressures up to 400 MPa. The estimated expanded uncertainty (at a coverage factor of  $k = 2$ ) in the range of validity of the correlation varies depending on the temperature and pressure, from 0.2 % to 4 %. In the near critical region, the uncertainty is expected to be larger and may exceed 4 %. The correlation behaves in a physically reasonable manner when extrapolated up to 750 K, however care should be taken when using the correlation outside of the validated range.

Key words: thermal conductivity; transport properties; xenon.

---

<sup>a)</sup> Author to whom correspondence should be addressed

## 1 Introduction

In a series of recent papers, new reference correlations for the thermal conductivity of some simple fluids [1-4], hydrocarbons [5-13], alcohols [14], and refrigerants [15-17] were reported. In this paper, the methodology adopted in the aforementioned papers is extended to developing a new reference correlation for the thermal conductivity of xenon.

The currently employed reference correlation for the thermal conductivity of xenon was developed by Hanley et al. [18] in 1974; it is based on the corresponding-states principle and covers a temperature range from about the triple point to 500 K and pressures up to 20 MPa, with an overall uncertainty of 6 %, increasing to 15 % for the critical region. The only other available correlation is the corresponding-states model developed by Huber [19] and implemented in REFPROP v10.0 [20]; with 5 % uncertainty for the gas-phase thermal conductivity and 3 % for the liquid-phase thermal conductivity over temperatures from (170 – 235) K at pressures up to 50 MPa.

The analysis that will be described here is based on the most recent theoretical advances, as well as the best available experimental data for thermal conductivity. Thus, a prerequisite to the analysis is a critical assessment of the experimental data. For this purpose, two categories of experimental data are defined: primary data, employed in the development of the correlation, and secondary data, used simply for comparison purposes. According to the recommendation adopted by the Subcommittee on Transport Properties (now known as The International Association for Transport Properties) of the International Union of Pure and Applied Chemistry, the primary data are identified by a well-established set of criteria [21]. These criteria have been successfully employed to establish standard reference values for the viscosity and thermal conductivity of fluids over wide ranges of conditions, with uncertainties in the range of 1 %. However, in many cases, such a narrow definition unacceptably limits the range of the data representation. Consequently, within the primary data set, it is also necessary to include results that extend over a wide range of conditions, albeit with a higher uncertainty, provided they are consistent with other lower uncertainty data or with theory. In all cases, the uncertainty claimed for the final recommended data must reflect the estimated uncertainty in the primary information.

## 2 The Correlation

The thermal conductivity  $\lambda$  can be expressed as the sum of three independent contributions, as

$$\lambda(\rho, T) = \lambda_0(T) + \Delta\lambda(\rho, T) + \Delta\lambda_c(\rho, T), \quad (1)$$

where  $\rho$  is the density,  $T$  is the temperature, and the first term,  $\lambda_0(T) = \lambda(0, T)$ , is the contribution to the thermal conductivity in the dilute-gas limit, where only two-body molecular interactions occur. The final term,  $\Delta\lambda_c(\rho, T)$ , the critical enhancement, arises from the long-range density fluctuations that occur in a fluid near its critical point, which contribute to the divergence of the thermal conductivity at the critical point. Finally, the term  $\Delta\lambda(\rho, T)$ , the residual property, represents the contribution of all other effects to the thermal conductivity of the fluid at elevated densities.

Table 1 summarizes, to the best of our knowledge, the theoretical predictions/estimations, as well as the experimental measurements of the thermal conductivity of xenon reported in the literature and the uncertainties given by the original authors. As early as 1962, based on kinetic-theory calculations, Svehla [22] proposed atmospheric-pressure thermal conductivity values in the temperature range of (100 – 5000) K. Subsequently, in 1967, Hanley and Childs [23] employed a potential function and its parameters to correlate kinetic theory with experimental data and calculated dilute-gas values, covering the temperature range (100 – 1000) K. However, the first empirical correlation for the thermal conductivity of xenon, based on the corresponding-states principle, and valid from the triple point to 500 K and up to 20 MPa, was proposed in 1974 by Hanley et al. [18].

In 1976, Rabinovich et al. [24] employed various available equations of state for xenon to perform approximate calculations of its thermodynamic functions, and published a series of recommended tables, including values for thermal conductivity that cover the temperature range (170 – 1300) K and pressure range (0.1 – 100) MPa. In a paper published in 1980, Vargaftik and Vasilevskaya [25] reviewed high-temperature experimental data, and subsequently employed them to develop a power-law equation for the prediction of xenon’s thermal conductivity at atmospheric pressure and temperatures ranging from (800 – 5000) K.

In 1983, based on the corresponding-states principle, Najafi et al. [26] (also shown in the work of Kestin et al. [27]) proposed a new correlation, valid at the dilute-gas limit and at temperatures (165 – 2000) K, with an uncertainty of up to 2 %. Subsequently, in 1990, Bich et al. [28] employed kinetic theory to generate reference values for the thermal conductivity of xenon from the triple point to 5000 K at the dilute-gas limit, as well as at atmospheric pressure, with an uncertainty ranging from (0.3 – 2) % at the highest temperatures.

In 2017, Hellmann et al. [29] produced reference values for the dilute gas over a temperature range (100 – 5000) K with an uncertainty of (0.07 – 0.28) %, based on an *ab initio* intermolecular potential energy and related spectroscopic and thermophysical-properties data for xenon.

In 2020, the combined use of experimental viscosity ratios together with *ab initio* calculations for helium has driven significant improvements in the description of dilute-gas transport properties [30]. Hence, Xiao et al. [30] first used the *ab initio* calculations of Cencek et al. [31] and the recommended viscosity ratios of Berg and Moldover [32] to update previous measurements of xenon’s transport properties, performed by May et al. [33]. Subsequently, they used these improved values to get improved reference correlations for the dilute-gas transport properties of xenon and 9 other gases. The new reference dilute-gas thermal conductivity correlation for xenon covers the temperature range from (100 – 5000) K with a standard uncertainty of 0.11 % (at a coverage factor of  $k = 1$ ), and it will form the dilute-gas thermal conductivity contribution of xenon in this work. We note that the uncertainties in Xiao et al. [30] are expressed as standard uncertainties corresponding to a coverage factor of  $k = 1$ ; in this work all uncertainties discussed are combined expanded uncertainties with a coverage factor of  $k = 2$ .

**Table 1** Thermal conductivity theoretical predictions and measurements of xenon.

1 <sup>st</sup> author	Year Publ.	Ref.	Technique employed <sup>a</sup>	Purity (%)	Uncertainty (%)	No. of data	Temperature range (K)	Pressure range (MPa)
<b>Reference Correlations/Values</b>								
Xiao	2020	[30]	Dil. Gas Reference Cor.	-	0.2	-	100 - 5000	0
Hellmann	2017	[29]	Recommended Values	-	0.07 - 0.28	109	100 - 5000	0
Bich	1990	[28]	Recommended Values	-	0.3 – 2.0	92	165 - 5000	0
Najafi	1983	[26]	CS Correlation	-	2.0	-	165 - 2000	0
Vargaftik	1980	[25]	Recommended Equation	-	3.0 – 6.0	-	800 - 5000	0.1
Rabinovich	1976	[24]	Recommended Values	-	na	1800	170 - 1300	0.1 - 100
Hanley	1974	[18]	CS Correlation	-	6.0	47	170 - 500	0.1 - 20
Hanley	1967	[23]	Kinetic Theory Calc.	-	5.0	91	100 - 1000	0
Svehla	1962	[22]	Kinetic Theory Calc.	-	na	50	100 - 5000	0.1
<b>Primary Data</b>								
Assael	1981	[34]	THW2	99.997	0.2	15	307 - 310	0.6 - 4.6
Kestin	1980	[35]	THW2	99.995	0.3	19	300 - 303	0.5 - 5.2
Vidal	1979	[36]	CC	na	1.0	5	298	0.1 - 400
Tufeu	1971	[37]	CC	na	1.0	66	303 - 606	0.1 - 95
Ikenberry	1963	[38]	CC	ResGrad	2.0	68	170 - 235	2 - 50
<b>Secondary Data</b>								
Jody	1976	[39]	HWThDC	99.995	2.0	Eqn	500 - 2400	0.1
Shashkov	1976	[40]	HW	99.9	1.5	7	194 - 272	0.1
Bakulin	1975	[41]	CC	na	0.7	21	400 - 1400	0.1
Stefanov	1975	[42]	HWThDC	na	3.0	Eqn	1100 – 2200	0.1
Voshchinin	1975	[43]	CC	na	4.0	6	600 - 1100	0.1
Springer	1973	[44]	HWThDC	na	3.0	Eqn	1000 - 1500	0.1
Saxena	1971	[45]	HWThDC	>99	1.5	3	313 - 366	0.1
Vargaftik	1971	[46]	SHW	na	1.5	18	298 - 1179	0.1
Saxena	1969	[47]	HWThDC	>99	1.5	12	373 - 1473	0.1
Matula	1968	[48]	ShockTube	na	10 - 20	Eqn	1400 - 5000	0.1
Gambhir	1967	[49]	HWThDC	>99	1.5	4	303 - 364	0.1
Gandhi	1967	[50]	HWThDC	>99	1.5	4	303 - 363	0.1
Srivastava	1960	[51]	HWThDC	na	2.0	2	303, 318	0.1
Zaitseva	1959	[52]	HW	na	3.0	7	306 - 794	0.1
Kannuluik	1952	[53]	HWThDC	na	1.0	5	194 - 579	0.1
Thornton	1960	[54]	Sh.Kath.	>99	2.2	1	291	0.1
Keyes	1955	[55]	CC	na	5.0	10	171 - 273	0.1 – 1.1
Curie	1931	[56]	CSph	99.9	na	1	273	0.1

<sup>a</sup> CC, Concentric Cylinders; CSph, Concentric Spheres; CS, Corresponding States; HW, Hot Wire; HWThDC, Hot-Wire Thermal Diffusion Column; Sh.Kath, Shakespear katharometer; SHW, Short Hot Wire; THW2, Transient Hot Wire with 2 Pt wires; na, not available; Eqn, Equation.

The most accurate measurements of the thermal conductivity of xenon were performed by Assael et al. [34] and Kestin et al. [35] in transient hot-wire instruments with 2 Pt wires in an absolute manner, backed by a full theory, with uncertainties of 0.2 % and 0.3 %, respectively. The measurements of Assael et al. [34] were obtained in the temperature range (307 – 310) K and up to 4.6 MPa, while those of Kestin et al. [35] were obtained in the temperature range (300 – 303) K and up to 5.2 MPa. Those two sets were part of the primary data sets.

In 1979 Vidal et al. [36] employed an absolute concentric-cylinders instrument with a 1 % uncertainty at 298 K and up to a pressure of 400 MPa to measure the thermal conductivity of xenon. This set is included in the primary data set. We note that some of these measurements were also reproduced by Tufeu et al. [57], in a very small graph, and the full set of measurements, together with measurements of other investigators, were also reproduced by Le Neindre et al. [58]. This instrument was also employed earlier by Tufeu et al. [37] to perform measurements in a wider temperature range, i.e. (303 – 606) K and up to 95 MPa. Moreover, the same type of instrument was employed successfully by Ikenberry and Rice [38] at very low temperatures and pressures up to 50 MPa, with an uncertainty of 2 %. Regardless of this higher value of uncertainty, this set was included in the primary data set, as it extends to low temperatures and high pressures.

A concentric-cylinders instrument was employed by Bakulin et al. [41] at atmospheric pressure and high temperatures, with an uncertainty of 0.7 %. However, this set was found to be about 5 % higher than the values calculated by the very accurate correlation of Xiao et al. [30], and thus was not included in the primary data set. In addition, the atmospheric-pressure measurements of Shashkov et al. [40] performed in a hot-wire instrument at low temperatures, and those of Vargaftik and Yakush [46] with a short hot-wire instrument at high temperatures both showed deviations of 2.1 % and 3.5 %, respectively from the correlation of Xiao et al. [30], and therefore these two sets of measurements were not included in the primary data set. This difference is probably attributed to the very low value of thermal conductivity that xenon exhibits, which makes its measurement more difficult.

Other measurements were also not included in the primary data set. These measurements were all performed at or very near atmospheric pressure and contribute little to the development of the new correlation, as this is based on the very accurate dilute-gas values obtained from kinetic theory. Moreover, the hot-wire thermal diffusion column technique was employed by Saxena and Tondon [45], Saxena and Saxena [47], Gambhir et al. [49], Gandhi and Saxena [50], and Srivastava and Barua [51], with a 500- $\mu\text{m}$  Pt wire in the center, by Springer and Wingeier [44] with a 1000- $\mu\text{m}$  W wire, by Jody et al. [39] with a 1200- $\mu\text{m}$  W wire, by Kannuluik and Carman [53] with a 1500- $\mu\text{m}$  wire, and by Stefanov [42]. This technique requires calibration, and wire limitations become important in gases of very low conductivity such as xenon [53]. Hence, measurements performed by the hot-wire thermal diffusion column technique were not considered as primary data. Also, the atmospheric-pressure measurements of Matula [48], performed with an uncertainty of 10 % – 20 %, the concentric-cylinders measurements of Voshchinin et al. [43] performed with a 4 % uncertainty, and the much earlier measurements of

Zaitseva [52], Thornton [54], and Curie and Lepape [56], were considered as secondary measurements because of their higher uncertainty.

Figures 1 and 2 show the ranges of the primary measurements outlined in Table 1, and the phase boundary may be seen as well. The development of the correlation requires densities; in 2006, Lemmon and Span [59] developed an accurate, wide-ranging equation of state that is valid from the triple point up to 750 K and 700 MPa. The equation of state has an uncertainty in density of 0.2 % up to 100 MPa (excluding the critical region), rising to 1 % at higher pressures. We also adopt the values for the critical point from their equation of state; the critical temperature,  $T_c$ , and the critical density,  $\rho_c$ , are 289.733 K and 1102.8612 kg·m<sup>-3</sup>, respectively [59]. The triple-point temperature given by Lemmon and Span is 161.405 K. We here adopt the value of 161.406 K given in 2005 by Hill and Steele [60] and recently confirmed by Steur et al.[61]

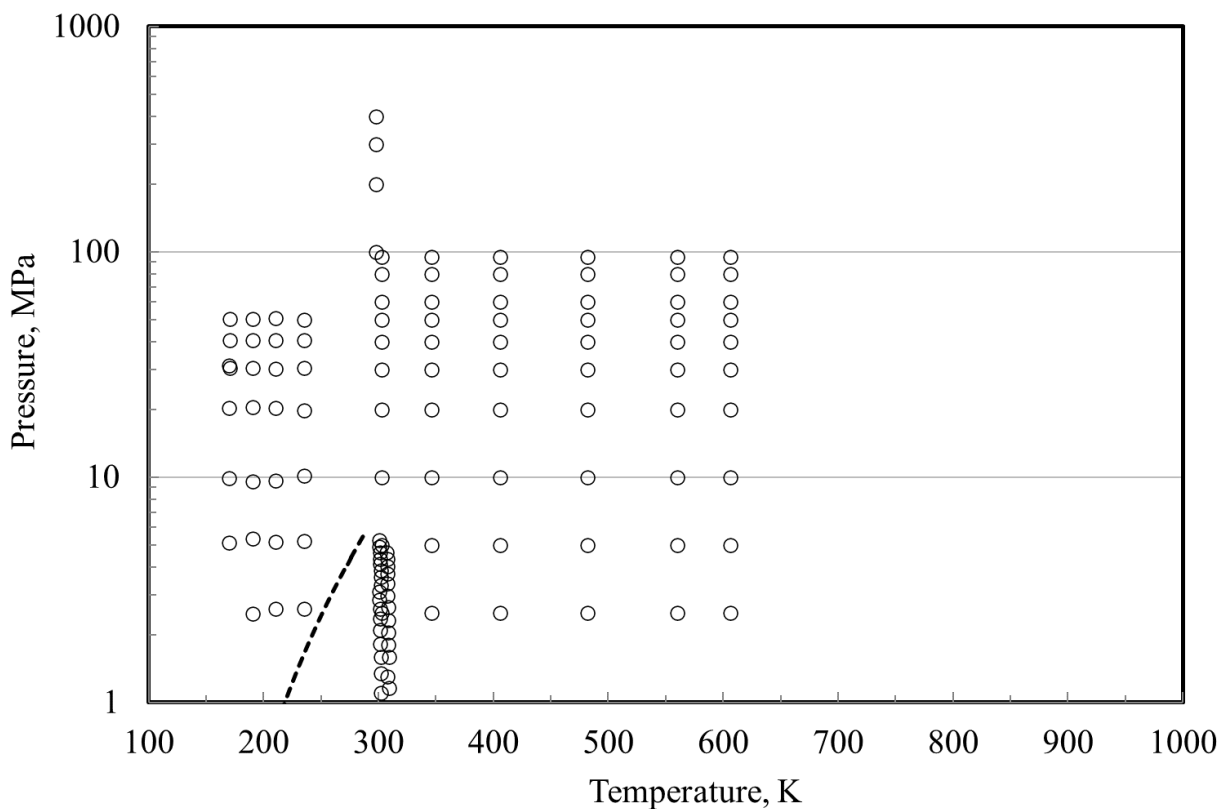


**FIG. 1** Temperature-pressure ranges of the primary experimental thermal conductivity data for xenon. Dilute-gas values from the reference correlation of Xiao et al.[30] are also shown (temperature restricted to 1000 K, as in the region up to 5000 K only dilute-gas values exist). (–) saturation curve.

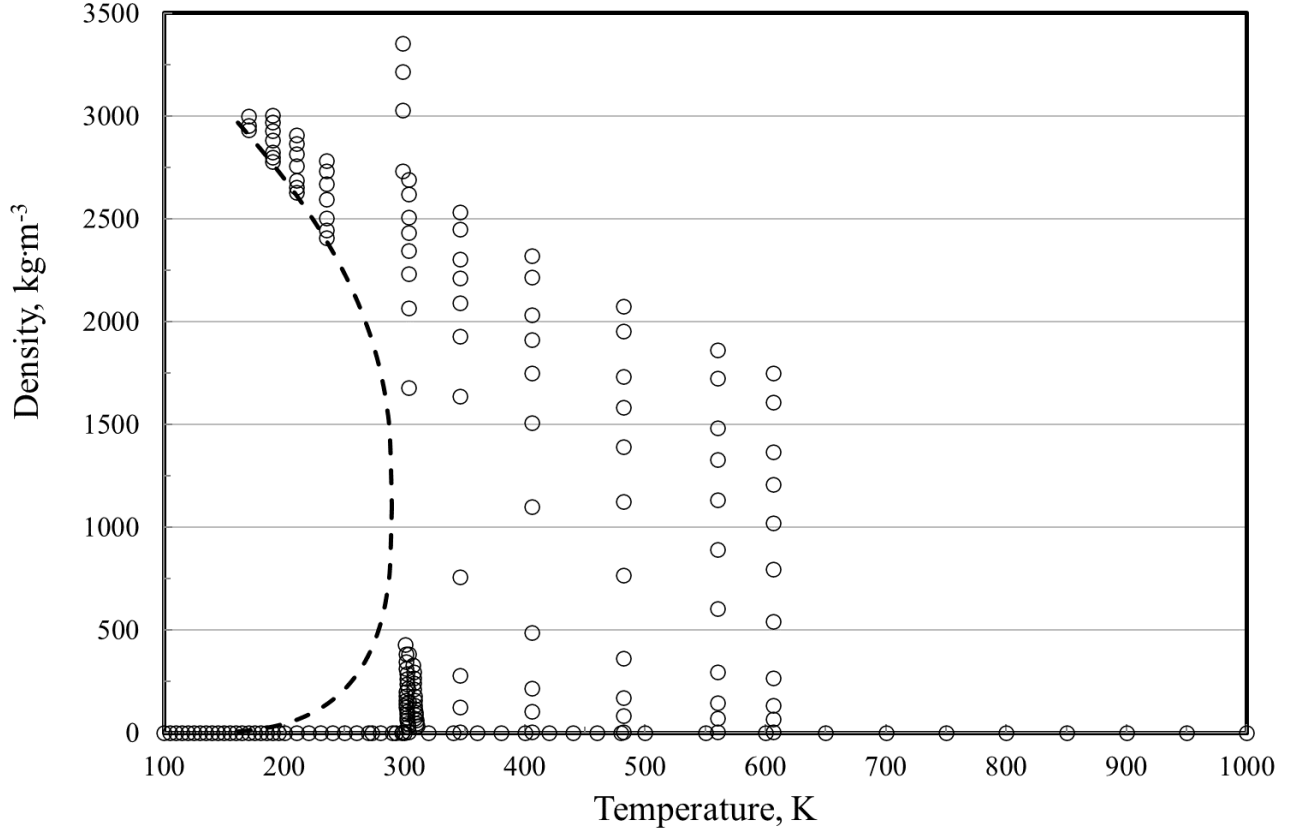


**FIG. 2** Temperature-density ranges of the primary experimental thermal conductivity data for xenon. Dilute-gas values from the reference correlation of Xiao et al. [30] are also shown (temperature restricted to 1000 K, as in the region up to 5000 K only dilute-gas values exist). (–) saturation curve.

## 2.1 The dilute-gas limit

The dilute-gas limit thermal conductivity,  $\lambda_0(T)$  in  $\text{mW}\cdot\text{m}^{-1}\cdot\text{K}^{-1}$ , can be analyzed independently of all other contributions in Eq. 1. As already discussed in the previous section, in 2020, the combined use of experimental viscosity ratios together with *ab initio* calculations for helium has driven significant improvements in the description of dilute-gas transport properties [30]. Hence, Xiao et al. [30] first used the *ab initio* calculations of Cencek et al. [31] and the recommended viscosity ratios of Berg and Moldover [32] to update previous measurements of xenon's transport properties, made by May et al. [33]. Subsequently, they used these improved values to get better reference correlations for the dilute-gas transport properties of xenon and 9 other gases. The new reference dilute-gas thermal conductivity correlation for xenon covers the temperature range from 100 K to 5000 K with a combined expanded uncertainty of 0.2 % and will form the dilute-gas viscosity contribution of xenon in this work. The dilute-gas limit thermal conductivity,  $\lambda_0$  given by Xiao et al. [30] is,

$$\lambda_0(T) = \lambda_0(298.15 \text{ K}) \exp \left\{ \sum_{i=1}^{11} b_i \left( \ln \left[ \frac{T}{298.15 \text{ K}} \right] \right)^i \right\}. \quad (2)$$

For the thermal conductivity at 298.15 K,  $\lambda_0(298.15 \text{ K})$ , the value of  $5.4666 \text{ mW}\cdot\text{m}^{-1}\cdot\text{K}^{-1}$  is proposed [30]. The coefficients  $b_i$  (-), are shown in Table 2.

**Table 2** Coefficients  $b_i$  of Eq. 2 [30].

$i$	$b_i$
1	$9.655\ 20 \times 10^{-1}$
2	$-5.123\ 53 \times 10^{-2}$
3	$-6.709\ 13 \times 10^{-2}$
4	$2.889\ 38 \times 10^{-2}$
5	$9.255\ 46 \times 10^{-3}$
6	$-9.721\ 75 \times 10^{-3}$
7	$1.693\ 64 \times 10^{-3}$
8	$9.968\ 03 \times 10^{-4}$
9	$-6.104\ 66 \times 10^{-4}$
10	$1.333\ 27 \times 10^{-4}$
11	$-1.098\ 58 \times 10^{-5}$

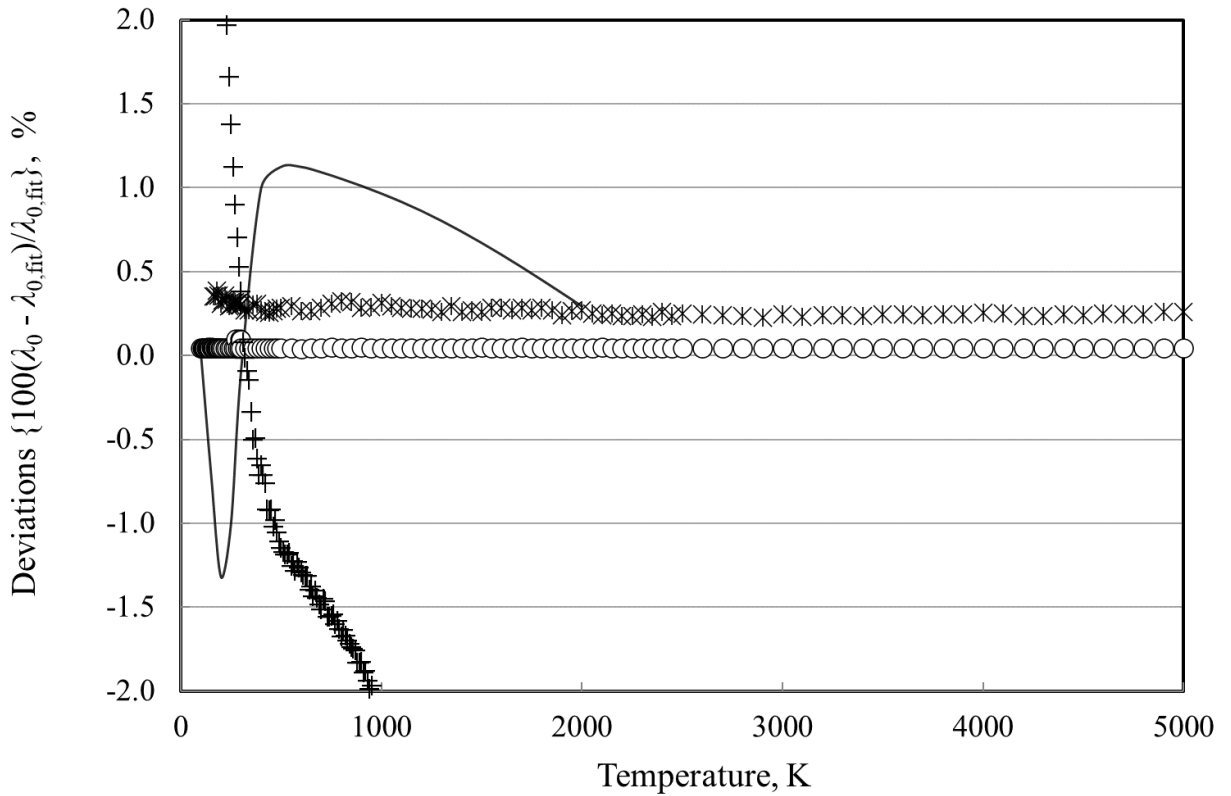


**FIG. 3** Percentage deviations of the dilute-gas values of the thermal conductivity of xenon from the values calculated by Eq. 2. Hellmann et al. [29] (O), Bich et al. [28] (\*), Najafi et al. [26] (—), Hanley and Childs [23] (+).

Figure 3 shows the percentage deviations from the dilute-gas thermal conductivity correlation of Eq. 2, as a function of temperature. The *ab initio*, 2017 calculated values of Hellmann et al. [29] agree with the proposed correlation within 0.05 %, while the 1990 recommended dilute-gas values of Bich et al. [28], quoted with an uncertainty of 0.3 % to 2 %, are well within the mutual uncertainties. In the same figure, we included the dilute-gas corresponding-states correlation of Najafi et al. [26], quoted with an uncertainty of 2%; this correlation is also within the mutual uncertainties of the two correlations. Finally, the only other set of recommended dilute-gas thermal conductivity values is that of Hanley and Childs [23] in 1967. These values, calculated from kinetic theory and measurements, are quoted with a 5 % uncertainty, increased in the ranges (100 – 270) K and (980 – 1000) K, as they were extrapolated values. These values are also within the mutual uncertainties of the two correlations.

Hence Eq. 2, proposed by Xiao et al. [30], represents the dilute-gas limit thermal conductivity of xenon with an uncertainty of 0.2 % over the temperature range (100 – 5000) K.

## 2.2 The residual term

The thermal conductivities of pure fluids exhibit an enhancement over a large range of densities and temperatures around the critical point and become infinite at the critical point. This behavior can be described by models that produce a smooth crossover from the singular behavior of the thermal conductivity asymptotically close to the critical point to the residual values far away from the critical point [62, 63]. The density-dependent terms for thermal conductivity can be grouped according to Eq. (1) as  $[\Delta\lambda(\rho, T) + \Delta\lambda_c(\rho, T)]$ . To assess the critical enhancement theoretically, we need to evaluate, in addition to the dilute-gas thermal conductivity, the residual thermal-conductivity contribution. The procedure adopted during this analysis used ODRPACK [64] to fit all the primary data simultaneously to the residual thermal conductivity and the critical enhancement, while maintaining the values of the dilute-gas thermal-conductivity already obtained. The density values employed were obtained by the equation of state of Lemmon and Span [59], valid from the triple point up to 750 K and up to 700 MPa. The primary data were weighted in inverse proportion to the square of their uncertainty.

The residual thermal conductivity was represented with a polynomial in temperature and density:

$$\Delta\lambda(\rho, T) = 1000 \sum_{i=1}^5 [(B_{1,i} + B_{2,i}(T/T_c))(\rho/\rho_c)^i]. \quad (3)$$

Coefficients  $B_{1,i}$  and  $B_{2,i}$  are shown in Table 3.

**Table 3** Coefficients of Eq. 7 for the residual thermal conductivity of xenon.

$i$	$B_{1,i}$ (mW·m <sup>-1</sup> ·K <sup>-1</sup> )	$B_{2,i}$ (mW·m <sup>-1</sup> ·K <sup>-1</sup> )
1	$0.694\ 552 \times 10^{-2}$	$-0.732\ 747 \times 10^{-4}$
2	$0.876\ 111 \times 10^{-2}$	$-0.268\ 366 \times 10^{-2}$
3	$-0.119\ 900 \times 10^{-1}$	$0.563\ 598 \times 10^{-2}$
4	$0.684\ 476 \times 10^{-2}$	$-0.314\ 076 \times 10^{-2}$
5	$-0.102\ 229 \times 10^{-2}$	$0.605\ 394 \times 10^{-3}$

### 2.3 The critical enhancement term

The theoretically based crossover model proposed by Sengers and coworkers [62, 63] is complex and requires solution of a quartic system of equations in terms of complex variables. A simplified crossover model has been proposed by Olchowy and Sengers [65]. The critical enhancement of the thermal conductivity from this simplified model is given by

$$\Delta\lambda_c = \frac{\rho C_p R_D k_B T}{6\pi\bar{\eta}\xi} (\bar{\Omega} - \bar{\Omega}_0), \quad (4)$$

with

$$\bar{\Omega} = \frac{2}{\pi} \left[ \left( \frac{C_p - C_v}{C_p} \right) \arctan(\bar{q}_D \xi) + \frac{C_v}{C_p} \bar{q}_D \xi \right] \quad (5)$$

and

$$\bar{\Omega}_0 = \frac{2}{\pi} \left[ 1 - \exp \left( - \frac{1}{(\bar{q}_D \xi)^{-1} + (\bar{q}_D \xi \rho_c / \rho)^2 / 3} \right) \right]. \quad (6)$$

In Eqs. 4-6,  $\bar{\eta}$  is the viscosity, and  $C_p$  and  $C_v$  are the isobaric and isochoric specific heat, respectively, obtained from the equation of state, and  $k_B$  is the Boltzmann constant. Note that when base SI mass units are used for all quantities in Eq. (4), the units of thermal conductivity are W·m<sup>-1</sup>·K<sup>-1</sup>, and the result must be divided by a factor of 1000 before addition to Eq.(2, 3) which are in mW·m<sup>-1</sup>·K<sup>-1</sup>. The correlation length,  $\xi$  (m), is given by:

$$\xi = \xi_0 \left( \frac{p_c \rho}{\Gamma \rho_c^2} \right)^{\nu/\gamma} \left[ \left. \frac{\partial \rho(T, \rho)}{\partial p} \right|_T - \left( \frac{T_{\text{ref}}}{T} \right) \left. \frac{\partial \rho(T_{\text{ref}}, \rho)}{\partial p} \right|_T \right]^{\nu/\gamma}. \quad (7)$$

As already mentioned, the coefficients  $B_{1,i}$  and  $B_{2,i}$  in Eq. 7 were fitted with ODRPACK [64] to the primary data for the thermal conductivity of xenon. This crossover model requires the universal amplitude,  $R_D = 1.02$  (-), and the universal critical exponents,  $\nu = 0.63$  and  $\gamma = 1.239$ , as well as the

system-dependent amplitudes  $\Gamma$  and  $\zeta_0$ . For this work, we adopted the values  $\Gamma = 0.058$  (–) and  $\zeta_0 = 0.182 \times 10^{-9}$  m, using the universal representation of the critical enhancement of the thermal conductivity by Perkins et al. [66]. Moreover, for the remaining parameter, i.e. the effective cutoff wavelength, we employed the fixed value also given by Perkins et al. [66] as  $q_D^{-1} = 0.479 \times 10^{-9}$  m. The viscosity required for Eq. 4 was obtained by the recent correlation of Velliadou et al. [67]. The reference temperature  $T_{\text{ref}}$ , far above the critical temperature where the critical enhancement is negligible, was calculated by  $T_{\text{ref}} = (3/2) T_c$  [68], which for xenon is 434.6 K. For conversion between mass and molar units, we use a molar mass of 131.293 g mol<sup>-1</sup>.

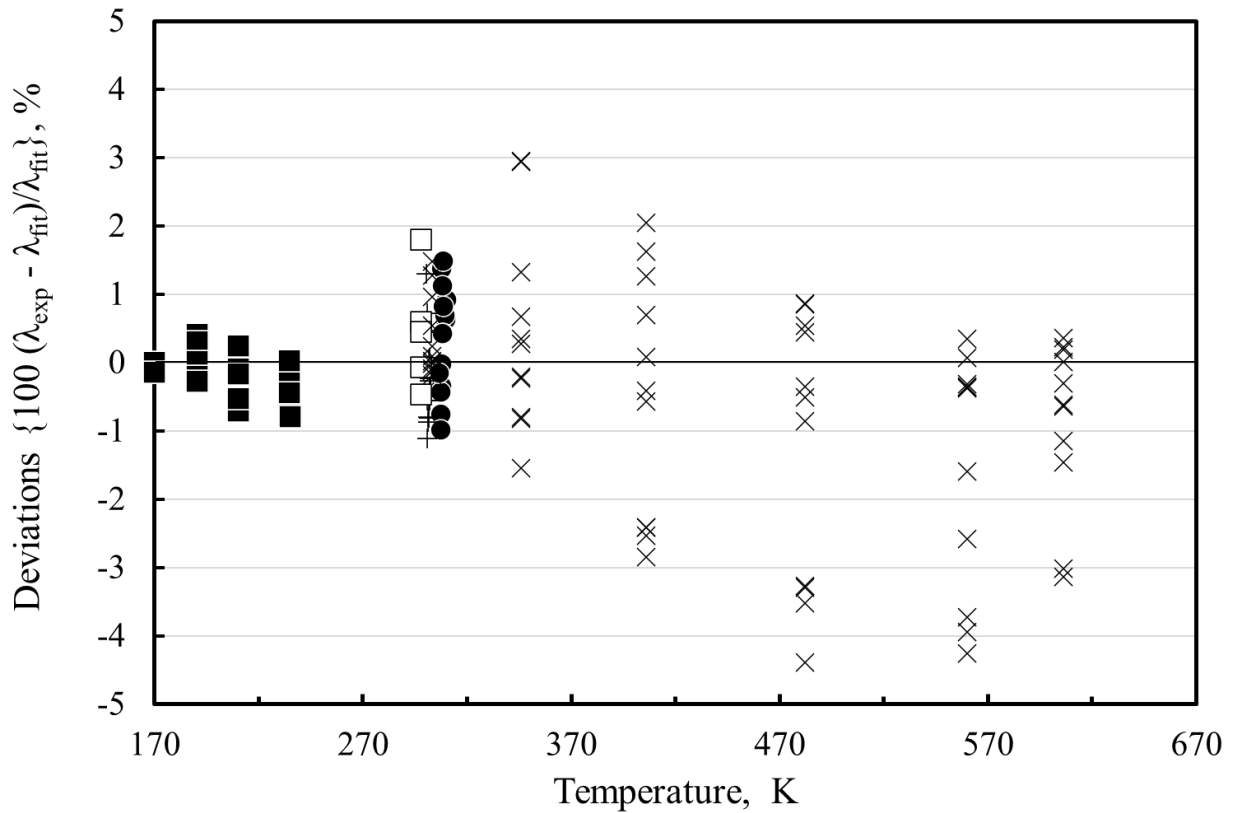
## 2.4 Comparison with data

Table 4 summarizes comparisons of the primary data with the correlation. We have defined the percent deviation as  $\text{PCTDEV} = 100(\lambda_{\text{exp}} - \lambda_{\text{fit}})/\lambda_{\text{fit}}$ , where  $\lambda_{\text{exp}}$  is the experimental value of the thermal conductivity and  $\lambda_{\text{fit}}$  is the value calculated from the correlation. Thus, the average absolute percent deviation (AAD) is found with the expression  $\text{AAD} = (\sum |\text{PCTDEV}|)/n$ , where the summation is over all  $n$  points, the bias percent is found with the expression  $\text{BIAS} = (\sum \text{PCTDEV})/n$ . The average absolute percent deviation of the fit is 0.87 %, and its bias is –0.29 %. Fig. 4 shows the percentage deviations of all primary thermal-conductivity data of xenon from the developed correlation, as a function of temperature, while Figs. 5 and 6 present the same deviations, but as a function of pressure and density, respectively. The deviations of the experimental data from the present correlation are within the mutual uncertainties, with only very few exceptions (from Tufeu et al., 4 points at 482 K and pressures (0.1 – 10) MPa, and 3 points at 560 K and pressures (0.1 – 5) MPa).

Based on comparisons with the primary data, we estimate the expanded uncertainty (at a 95 % confidence level) in thermal conductivity of the liquid at pressures up to 50 MPa, to be the same as the uncertainty of the data in that region, 2 %. As discussed earlier, the dilute-gas limit thermal conductivity has an expanded uncertainty of 0.2 % over the temperature range (100 – 5000) K. For the gas and supercritical fluid at temperatures below 345 K and pressures from 0.1 MPa up to 5 MPa the estimated expanded uncertainty is 1.5 %, rising to 2 % at pressures up to 400 MPa. For temperatures from (345 – 606) K the expanded uncertainty is 4 % at pressures up to 100 MPa. The correlation behaves in a physically realistic manner at temperatures up to 750 K ( the limit of the equation of state Lemmon and Span [59]) and we feel the correlation may be extrapolated to this limit, although the uncertainty will be larger. Additional experimental data at high temperatures and pressures are necessary to validate the correlation or make improved correlations possible in the future.

**Table 4** Evaluation of xenon's thermal-conductivity correlation for the primary data.

1 <sup>st</sup> Author	Year Publ.	Ref.	AAD (%)	BIAS (%)
Assael	1981	[34]	0.70	0.34
Kestin	1980	[35]	0.51	-0.19
Vidal	1979	[36]	0.67	0.45
Tufeu	1971	[37]	1.24	-0.55
Ikenberry	1963	[38]	0.32	-0.19
<b>Entire data set</b>			<b>0.87</b>	<b>-0.29</b>

**FIG. 4** Percentage deviations of primary experimental data of the thermal conductivity of xenon from the values calculated by the present model, as a function of temperature. Assael *et al.* [34] (●), Kestin *et al.* [35] (+), Vidal *et al.* [36], (□), Tufeu *et al.* [37] (x), and Ikenberry and Rice [38] (■).

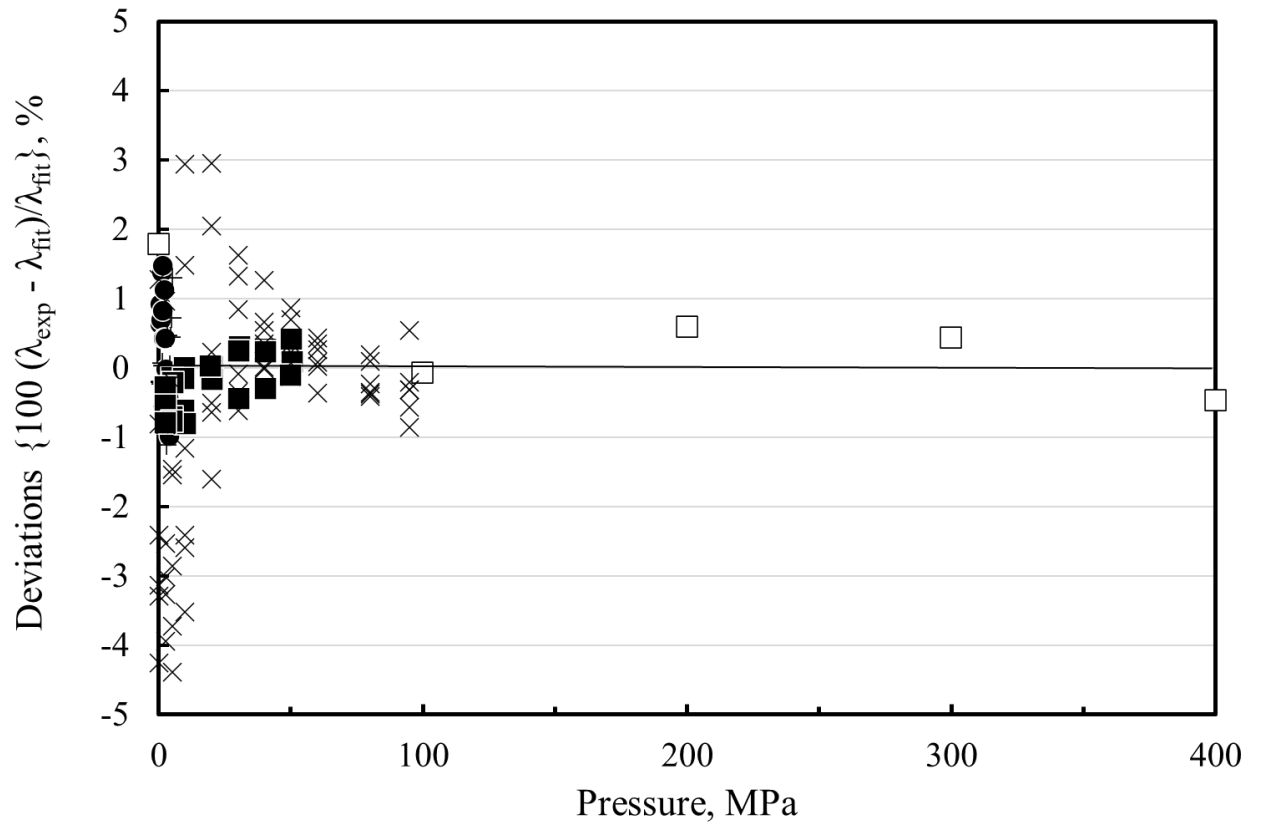


**FIG. 5** Percentage deviations of primary experimental data of the thermal conductivity of xenon from the values calculated by the present model, as a function of pressure. Assael *et al.* [34] (●), Kestin *et al.* [35] (+), Vidal *et al.* [36], (□), Tufeu *et al.* [37] (X), and Ikenberry and Rice [38] (■).

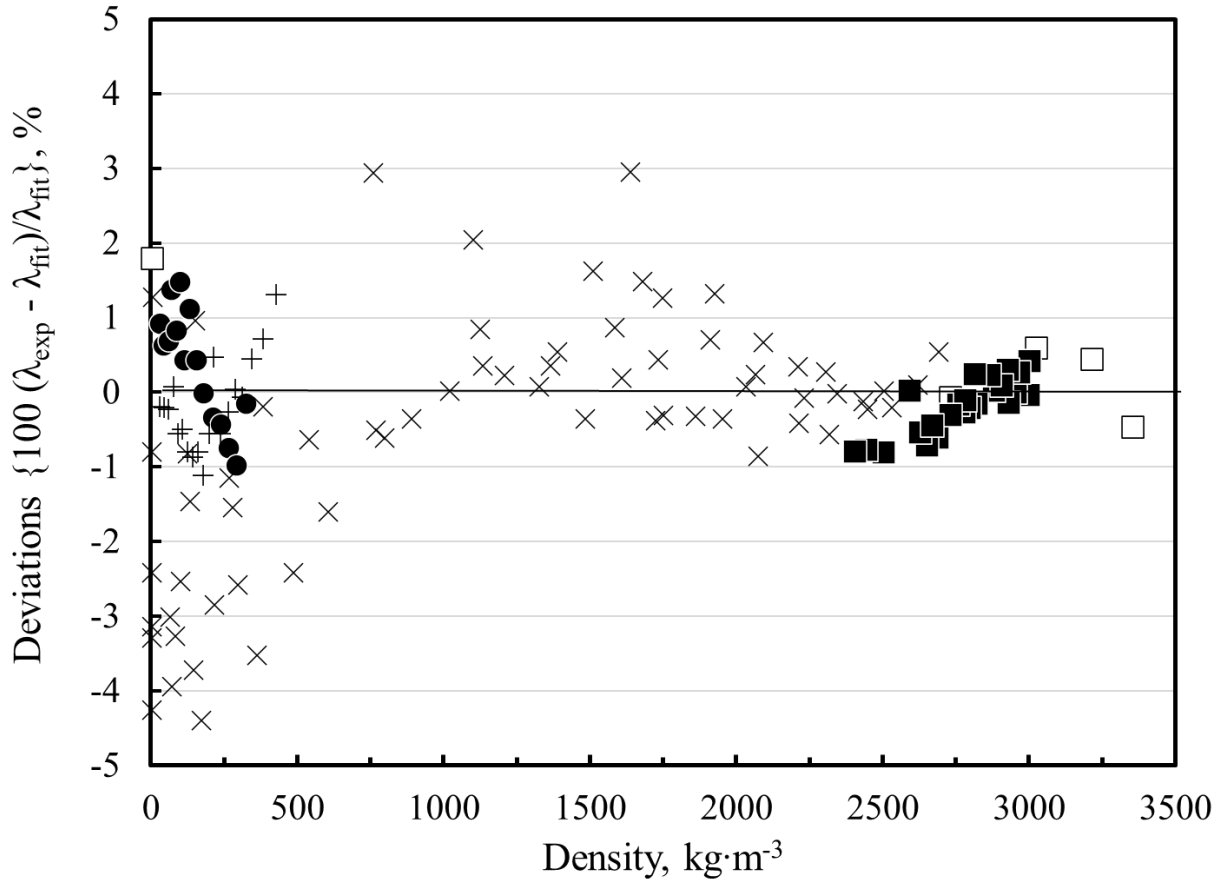


**FIG.6** Percentage deviations of primary experimental data of the thermal conductivity of xenon from the values calculated by the present model, as a function of density. Assael *et al.* [34] (●), Kestin *et al.* [35] (+), Vidal *et al.* [36], (□), Tufeu *et al.* [37] (X), and Ikenberry and Rice [38] (■).

Table 5 shows the average absolute percent deviation (AAD) and the bias for the secondary data. Furthermore, Fig. 7 shows the plot of the thermal conductivity of xenon as a function of temperature for different pressures as well as the saturated liquid and vapor values. This plot demonstrates the extrapolation behavior of the thermal conductivity correlation at temperatures that extend to the 750 K limit of the equation of state. Finally, the plot of Fig. 8 shows the thermal conductivity of xenon as a function of density for different temperatures, including the critical enhancement.

**Table 5** Evaluation of the xenon thermal-conductivity correlation for the secondary data.

1 <sup>st</sup> Author	Year Publ.	Ref.	AAD (%)	BIAS (%)
Jody	1976	[39]	1.34	1.08
Shashkov	1976	[40]	2.10	2.10
Bakulin	1975	[41]	4.24	4.24
Stefanov	1975	[42]	1.08	0.54
Voshchinin	1975	[43]	3.03	3.03
Springer	1973	[44]	1.03	-1.03
Saxena	1971	[45]	4.14	4.14
Vargaftik	1971	[46]	3.45	3.45
Saxena	1969	[47]	4.21	4.21
Matula	1968	[48]	11.08	-11.08
Gambhir	1967	[49]	3.87	3.43
Gandhi	1967	[50]	8.32	-3.40
Srivastava	1960	[51]	3.35	-3.35
Zaitseva	1959	[52]	10.18	-10.18
Kannuluik	1952	[53]	2.14	1.58
Thornton	1960	[54]	2.64	2.64
Keyes	1955	[55]	1.45	1.45
Curie	1931	[56]	2.58	2.58

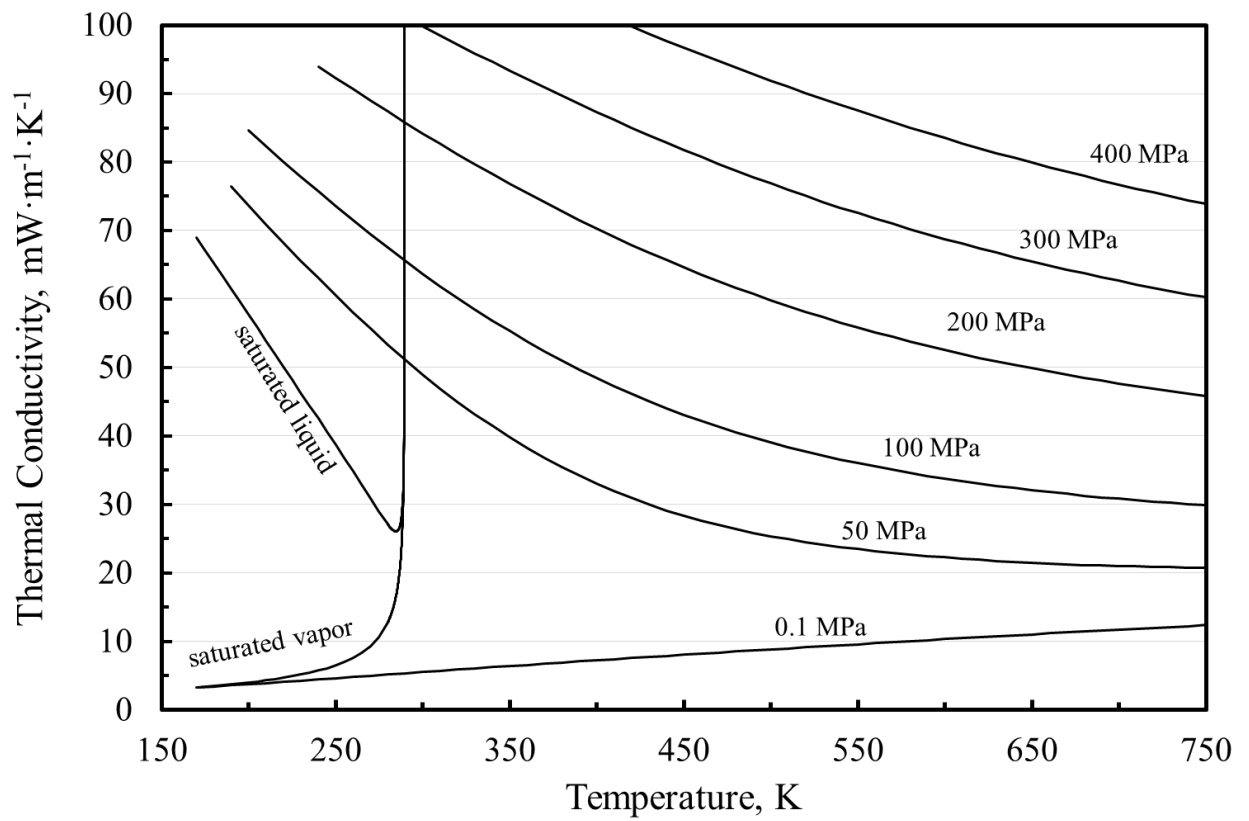


**FIG. 7** Thermal conductivity of xenon as a function of temperature for selected pressures.

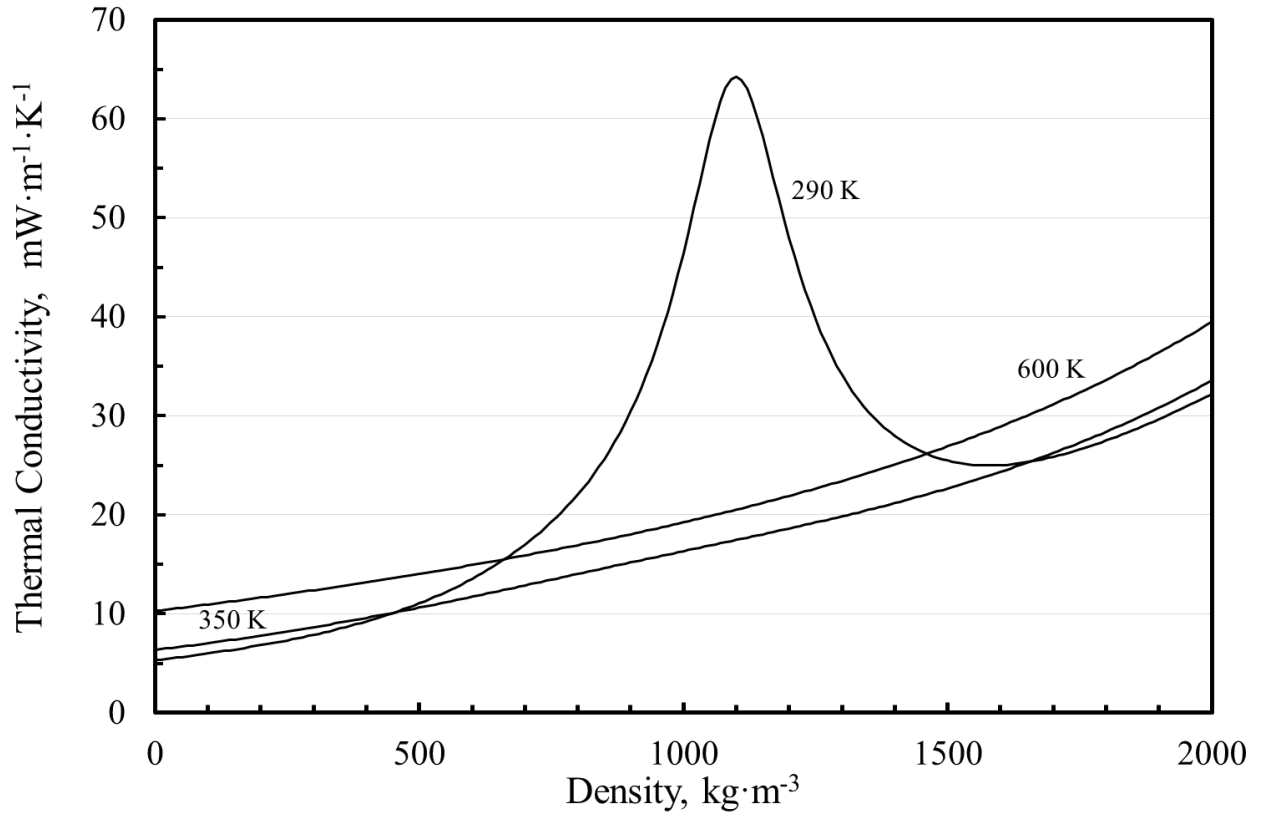


**FIG. 8** Thermal conductivity of xenon as a function of density for selected temperatures.

### 3. Recommended Values

In Table 6, thermal conductivity values are given along the saturation curve, calculated from the present scheme between (170 – 285) K, while in Table 7 thermal conductivity values are calculated from the present correlation, for temperatures between 200 K and 750 K, at selected pressures. Points denoted as solid occur at state points above the melting line [69]. Saturation pressure and saturation density values for selected temperatures, as well as the density values for the selected temperature and pressure, are obtained from the equation of state of Lemmon and Span [59]. For checking of computer calculations, for  $T = 300$  K at  $\rho = 1200.0$   $\text{kg}\cdot\text{m}^{-3}$ , the dilute-gas contribution from Eq. (6) is  $5.4993$   $\text{mW}\cdot\text{m}^{-1}\cdot\text{K}^{-1}$ , the residual contribution from Eq. (7) is  $11.0621$   $\text{mW}\cdot\text{m}^{-1}\cdot\text{K}^{-1}$ , and the contribution from the critical enhancement in Eqs. (8) – (11) is  $6.2061$   $\text{mW}\cdot\text{m}^{-1}\cdot\text{K}^{-1}$ , leading to a value for the thermal conductivity of  $22.7675$   $\text{mW}\cdot\text{m}^{-1}\cdot\text{K}^{-1}$ . At this same state point, the viscosity is  $57.059$   $\mu\text{Pa}\cdot\text{s}$  [67].

**Table 6** Thermal conductivity values of xenon along the saturation boundary, calculated by the present scheme.

$T$ (K)	$p$ (MPa)	$\rho_{\text{liq}}$ ( $\text{kg}\cdot\text{m}^{-3}$ )	$\rho_{\text{vap}}$ ( $\text{kg}\cdot\text{m}^{-3}$ )	$\lambda_{\text{liq}}$ ( $\text{mW}\cdot\text{m}^{-1}\cdot\text{K}^{-1}$ )	$\lambda_{\text{vap}}$ ( $\text{mW}\cdot\text{m}^{-1}\cdot\text{K}^{-1}$ )
170	0.13343	2908.8	12.88	68.99	3.25
190	0.34774	2768.4	31.19	61.48	3.74
210	0.75025	2614.9	64.37	53.92	4.34
230	1.41554	2441.5	120.07	46.34	5.18
250	2.42287	2235.4	212.13	38.71	6.49
270	3.86231	1962.2	376.62	30.93	9.26
285	5.30253	1607.3	655.30	26.07	17.04

**Table 7** Thermal conductivity values of xenon at selected temperatures and pressures, calculated by the present scheme.

$p$ (MPa)	$T$ (K)	$\rho$ ( $\text{kg}\cdot\text{m}^{-3}$ )	$\lambda$ ( $\text{mW}\cdot\text{m}^{-1}\cdot\text{K}^{-1}$ )	$p$ (MPa)	$T$ (K)	$\rho$ ( $\text{kg}\cdot\text{m}^{-3}$ )	$\lambda$ ( $\text{mW}\cdot\text{m}^{-1}\cdot\text{K}^{-1}$ )
0.1	200	8.032	3.76	100	200	3112.6	84.63
	250	6.372	4.65		250	2915.5	73.60
	300	5.291	5.53		300	2725.0	63.70
	350	4.526	6.40		350	2542.1	55.30
	400	3.956	7.24		400	2368.9	48.50
	450	3.514	8.06		450	2207.7	43.10
	500	3.161	8.84		500	2059.9	39.06
	550	2.873	9.60		550	1925.9	36.04
	600	2.633	10.33		600	1805.3	33.78
10	200	2762.2	61.56	200	200	solid	solid
	250	2375.5	44.13		250	3166.7	92.29
	300	1744.0	26.48		300	3023.2	84.21
	350	724.4	13.16		350	2888.3	76.82
	400	501.1	11.22		400	2761.5	70.30
	450	403.8	11.03		450	2642.7	64.61
	500	344.5	11.30		500	2531.6	59.84
	550	303.1	11.71		550	2428.2	55.87
	600	271.9	12.18		600	2331.9	52.58
40	200	2917	71.06	400	200	solid	solid
	250	2648	57.22		250	solid	solid
	300	2364	45.18		300	3351.3	112.82
	350	2069.2	35.68		350	3249.6	107.29
	400	1782.1	28.98		400	3154.1	101.87
	450	1528.3	24.54		450	3064.3	96.69
	500	1321.8	22.02		500	2979.7	91.89
	550	1160.4	20.54		550	2899.8	87.49
	600	1034.6	19.67		600	2824.3	83.50

#### 4. Conclusions

A new wide-ranging correlation for the thermal conductivity of xenon was developed based on critically evaluated experimental data and theoretical results. In the dilute-gas range, the correlation incorporates the very recent correlation of Xiao et al. [30], with an expanded uncertainty ( $k = 2$ ) of 0.2 % over the temperature range (100 – 5000) K. The expanded uncertainty (at a 95 % confidence level) in thermal conductivity of the liquid phase at pressures up to 50 MPa, is 2 %. For the gas and supercritical fluid at temperatures below 345 K and pressures from 0.1 MPa up to 5 MPa the estimated expanded uncertainty is 1.5 %, rising to 2 % at pressures up to 400 MPa. For temperatures from (345 – 606) K the expanded uncertainty is 4 % at pressures up to 100 MPa. The correlation is designed to be used with the equation of state of Lemmon and Span [59] that is valid from the triple point to 750 K. The thermal conductivity behaves in a physically realistic manner at temperatures up to 750 K and pressures to 400 MPa, and we feel the correlation may be extrapolated to this limit, although the uncertainty will be larger, and caution is advised.

#### 5. References

1. M.J. Assael, J.A.M. Assael, M.L. Huber, R.A. Perkins, Y. Takata, J. Phys. Chem. Ref. Data 40 (3), 033101 (2011)
2. M.J. Assael, I.A. Koini, K.D. Antoniadis, M.L. Huber, I.M. Abdulagatov, R.A. Perkins, J. Phys. Chem. Ref. Data 41 (2), 023104 (2012)
3. M.L. Huber, R.A. Perkins, D.G. Friend, J.V. Sengers, M.J. Assael, I.N. Metaxa, K. Miyagawa, R. Hellmann, E. Vogel, J. Phys. Chem. Ref. Data 41 (3), 033102 (2012)
4. M.L. Huber, E.A. Sykioti, M.J. Assael, R.A. Perkins, J. Phys. Chem. Ref. Data 45 (1), 013102 (2016)
5. M.J. Assael, S.K. Mylona, M.L. Huber, R.A. Perkins, J. Phys. Chem. Ref. Data 41 (2), 023101 (2012)
6. M.J. Assael, E.K. Michailidou, M.L. Huber, R.A. Perkins, J. Phys. Chem. Ref. Data 41 (4), 043102 (2012)
7. C.-M. Vassiliou, M.J. Assael, M.L. Huber, R.A. Perkins, J. Phys. Chem. Ref. Data 44 (3), 033102 (2015)
8. M.J. Assael, I. Bogdanou, S.K. Mylona, M.L. Huber, R.A. Perkins, V. Vesovic, J. Phys. Chem. Ref. Data 42 (2), 023101 (2013)
9. S.A. Monogenidou, M.J. Assael, M.L. Huber, J. Phys. Chem. Ref. Data 47, 013103 (2018)
10. A. Koutian, M.J. Assael, M.L. Huber, R.A. Perkins, J. Phys. Chem. Ref. Data 46, 013102 (2017)
11. M.J. Assael, A. Koutian, M.L. Huber, R.A. Perkins, J. Phys. Chem. Ref. Data 45 (3), 033104 (2016)

12. S.K. Mylona, K.D. Antoniadis, M.J. Assael, M.L. Huber, R.A. Perkins, *J. Phys. Chem. Ref. Data* 43, 043104 (2014)
13. M.J. Assael, T.B. Papalas, M.L. Huber, *J. Phys. Chem. Ref. Data* 46 (3), 033103 (2017)
14. E.A. Sykioti, M.J. Assael, M.L. Huber, R.A. Perkins, *J. Phys. Chem. Ref. Data* 42 (4), 043101 (2013)
15. R.A. Perkins, M.L. Huber, M.J. Assael, *J. Chem. Eng. Data* 61 (9), 3286 (2016)
16. C.M. Tsolakidou, M.J. Assael, M.L. Huber, R.A. Perkins, *J. Phys. Chem. Ref. Data* 46 (2), 023103 (2017)
17. S.A. Monogenidou, M.J. Assael, M.L. Huber, *J. Phys. Chem. Ref. Data* 47 (4), 043101 (2018)
18. H.J.M. Hanley, R.D. McCarty, W.M. Haynes, *J. Phys. Chem. Ref. Data* 3 (4), 979 (1974)
19. M.L. Huber, Models for viscosity, thermal conductivity, and surface tension of selected fluids as implemented in REFPROP v10.0, NISTIR 8209, doi:10.6028/NIST.IR.8209. (National Institute of Standards and Technology, Gaithersburg, MD, 2018)
20. E.W. Lemmon, I.H. Bell, M.L. Huber, M.O. McLinden, NIST Standard Reference Database 23, NIST Reference Fluid Thermodynamic and Transport Properties Database (REFPROP): Version 10.0. (2018)
21. M.J. Assael, A.E. Kalyva, S.A. Monogenidou, M.L. Huber, R.A. Perkins, D.G. Friend, E.F. May, *J. Phys. Chem. Ref. Data* 47 (2), 021501 (2018)
22. R. Svehla, Estimated viscosities and thermal conductivities of gases at high temperatures, NASA Technical Report R-132, Cleveland OH. (1962)
23. H.J.M. Hanley, G.E. Childs, The viscosity and thermal conductivity coefficients of dilute neon, krypton, and xenon, NBS Technical Note 352, U.S. Government Printing Office, Washington DC. (1967)
24. V.A. Rabinovich, A.A. Vasserman, V.I. Nedostup, L.S. Veksler, Thermophysical Properties of Neon, Argon, Krypton, and Xenon. (National Standard Reference Data Service of the USSR, Moscow, 1976)
25. N.B. Vargaftik, Y.D. Vasilevskaya, *J. Eng. Phys.* 39, 1217 (1980)
26. B. Najafi, E.A. Mason, J. Kestin, *Physica A* 119 (3), 387 (1983)
27. J. Kestin, K. Knierim, E.A. Mason, B. Najafi, S.T. Ro, M. Waldman, *J. Phys. Chem. Ref. Data* 13 (1), 229 (1984)
28. E. Bich, J. Millat, E. Vogel, *J. Phys. Chem. Ref. Data* 19 (6), 1289 (1990)
29. R. Hellmann, B. Jäger, E. Bich, *J. Chem. Phys.* 147, 034304 (2017)
30. X. Xiao, D. Rowland, S.Z.S. Al Ghafri, E.F. May, *J. Phys. Chem. Ref. Data* 49 (1), 013101 (2020)
31. W. Cencek, M. Przybytek, J. Komasa, J.B. Mehl, B. Jeziorski, K. Szalewicz, *J. Chem. Phys.* 136, 224303 (2012)
32. R.F. Berg, M.R. Moldover, *J. Phys. Chem. Ref. Data* 41 (4), 043104 (2012)
33. E.F. May, R.F. Berg, M.R. Moldover, *Int. J. Thermophys.* 28 (4), 1085 (2007)

34. M.J. Assael, M. Dix, A. Lucas, W.A. Wakeham, *J. Chem. Soc., Faraday Trans. I* 77, 439 (1981)
35. J. Kestin, R. Paul, A.A. Clifford, W.A. Wakeham, *Physica A* 100 (2), 349 (1980)
36. D. Vidal, R. Tufeu, Y. Garrabos, B. Le Neindre, "High Pressure Science and Technology", Eds. B. Vodar, and Ph. Marteau, Proc. of VIIth AIPART Vonference, Le Creusot, France July 30-August 3. (Pergamon Press, New York, 1979)
37. R. Tufeu, B. Le Neindre, P. Bury, *C. R. Acad. Sc. Paris* 273 B, 113 (1971)
38. L. Ikenberry, S.A. Rice, *J. Chem. Phys.* 39 (6), 1561 (1963)
39. B.J. Jody, S.C. Saxena, V.P.S. Nain, R.A. Aziz, *High Temp. Sci.* 8, 343 (1976)
40. A.G. Shashkov, N.A. Nesterov, V.M. Sudnik, V.I. Aleinikova, *Inzh.-Fiz. Zh.* 30, 671 (1976)
41. S.S. Bakulin, S.A. Ulybin, E.N. Zherdev, *Teplofiz. Vys. Temp.* 13, 760 (1975)
42. B. Stefanov, *J. Chem. Phys.* 63 (5), 2258 (1975)
43. A.A. Voshchinin, V.V. Kerzhentsev, E.L. Studnikov, L.V. Yakush, *Izv. Vyssh. Uchebn. Zaved. Energ.* 7, 88 (1975)
44. G.S. Springer, E.W. Wingeier, *J. Chem. Phys.* 59 (5), 2747 (1973)
45. S.C. Saxena, P.K. Tondon, *J. Chem. Eng. Data* 16 (2), 212 (1971)
46. N.B. Vargaftik, L.V. Yakush, *Inzh.-Fiz. Zh* 21, 491 (1971)
47. V.K. Saxena, S.C. Saxena, *J. Chem. Phys.* 51 (8), 3361 (1969)
48. R.A. Matula, *J. Heat Transfer* 90 (3), 319 (1968)
49. R.S. Gambhir, J.M. Gandhi, S.C. Saxena, *Indian J. Pure Appl. Phys.* 5, 457 (1967)
50. J.M. Gandhi, S.C. Saxena, *Mol. Phys.* 12, 57 (1967)
51. B.N. Srivastava, A.K. Barua, *J. Chem. Phys.* 32 (2), 427 (1960)
52. L.S. Zaitseva, *Zh. Tekh. Fiz.* 29, 497 (1959)
53. W.G. Kannuluik, E.H. Carman, *Proc. Phys. Soc. B* 65, 701 (1952)
54. E. Thornton, *Proc. Phys. Soc.* 76, 104 (1960)
55. F.G. Keyes, *Trans. ASME* 77, 1395 (1955)
56. H. Curie, A. Lepape, *J. Phys. Rad.* 2, 392 (1931)
57. R. Tufeu, D. Vidal, M. Lallemand, B. Le Neindre, *High Temp. High Press.* 11, 587 (1979)
58. B. Le Neindre, Y. Garrabos, R. Tufeu, *Physica A* 156 (1), 512 (1989)
59. E.W. Lemmon, R.J. Span, *J. Chem. Eng. Data* 51 (3), 785 (2006)
60. K.D. Hill, A.G. Steele, *Metrologia* 42 (4), 278 (2005)
61. P.P.M. Steur, P.M.C. Rourke, D. Giraudi, *Metrologia* 56 (1), 015008 (2019)
62. G.A. Olchowy, J.V. Sengers, *Phys. Rev. Lett.* 61 (1), 15 (1988)
63. R. Mostert, H.R. van Den Berg, P.S. van der Gulik, J.V. Sengers, *J. Chem. Phys.* 92 (9), 5454 (1990)
64. P.T. Boggs, R.H. Byrd, J.H. Rogers, R.B. Schnabel, User's referene guide for ODRPACK version 2.01, Software for weighted orthogonal distance regression, NISTIR 4834 (National Institute of Standards and Technology, Gaithersburg, MD, 1992)

65. G.A. Olchowy, J.V. Sengers, *Int. J. Thermophys.* 10 (2), 417 (1989)
66. R.A. Perkins, J.V. Sengers, I.M. Abdulagatov, M.L. Huber, *Int. J. Thermophys.* 34, 191 (2013)
67. D. Velliadou, K. Tasidou, K.D. Antoniadis, M.J. Assael, R.A. Perkins, M.L. Huber, *Int. J. Thermophys.* to be submitted (2021)
68. V. Vesovic, W.A. Wakeham, G.A. Olchowy, J.V. Sengers, J.T.R. Watson, J. Millat, *J. Phys. Chem. Ref. Data* 19 (3), 763 (1990)
69. A. Michels, C. Prins, *Physica* 28 (2), 101 (1962)